Construction and Building Materials 94 (2015) 90–104

Contents lists available at ScienceDirect

Construction and Building Materials

journal homepage: www.elsevier.com/locate/conbuildmat

Comparative study on effects of Class F fly ash, nano silica and silica fume on properties of high performance self compacting concrete

Mostafa Jalal [a,*], Alireza Pouladkhan [b], Omid Fasihi Harandi [c], Davoud Jafari [d]

[a] Young Researchers and Elites Club, Science and Research Branch, Islamic Azad University, Tehran, Iran
[b] Young Researchers and Elite Club, Najafabad Branch, Islamic Azad University, Najafabad, Esfahan, Iran
[c] Department of Civil Engineering, Najafabad Branch, Islamic Azad University, Isfahan, Iran
[d] Pishtazan Sanat Poolad Company, Isfahan, Iran

HIGHLIGHTS

- High performance self compacting concrete (HPSCC).
- Comparative effects of pozzolanic admixtures and nanopowder on properties of HPSCC.
- Strength and durability enhancement via blend of mineral admixtures and nanopowder.
- Energy saving in construction and building industry by traditional and new materials.

ARTICLE INFO

Article history:
Received 9 May 2013
Received in revised form 2 April 2015
Accepted 1 July 2015

Keywords:
High performance self compacting concrete (HPSCC)
Nano silica
Silica fume
Class F fly ash
Rheological properties
Mechanical properties
Transport properties
TGA

ABSTRACT

This paper presents the effects of some admixtures including silica nanoparticles, silica fume and Class F fly ash on different properties of high performance self compacting concrete (HPSCC). For this purpose, a fraction of Portland cement with the aim of cement content reduction was replaced different fractions of pozzolanic admixtures. The rheological properties of fresh concrete were observed through slump flow time and diameter and V-funnel flow time. Thermal properties were investigated via thermogravimetric analysis (TGA) test. Transport properties evaluated by water absorption, capillary absorption and chloride ion penetration tests. The results indicated that increase of fly ash content improves the rheological properties of HPSCC. The results also showed that mechanical and transport properties improved in the mixtures containing admixtures especially blend of silica nanoparticles and silica fume. It can also be concluded that higher amount of mineral admixtures combined with small fractions of nanopowders could be promising technique toward high performance concrete as a key material along with energy saving in construction and building technology.

1. Introduction

High performance concrete (HPC) offers high strength, better durability properties, and good construction. High strength is one of the important attributes of HPC. High strength concrete, according to American Concrete Institute Committee ACI 363 R [1], is the concrete which has specific compressive strength of 41 MPa or more at 28 days. The HPC offers significant economic and architectural advantages over NSC in similar situations, and is suited well for constructions that require high durability.

Self consolidating concrete (SCC) is a concrete which has little resistance to flow so that it can be placed and compacted under its own weight with no vibration effort, yet possesses enough viscosity to be handled without segregation or bleeding [2,3]. The most important advantage of SCC over conventional concrete is its flowability. Other advantages of using SCC include shorter construction periods, reduction in the labor cost, and better compaction in the structure especially in confined zones where compaction is difficult. SCC can also provide a better working environment by eliminating the vibration noise.

By combining the characteristics and advantages of HPC and SCC, high performance self-compacting concrete (HPSCC) can be produced which possesses the advantages in both forms of fresh and hardened concrete, i.e. while presenting higher strength and

* Corresponding author.
E-mail addresses: m.jalal.civil@gmail.com, mjalal@aut.ac.ir (M. Jalal).

http://dx.doi.org/10.1016/j.conbuildmat.2015.07.001
0950-0618/

durability, it has a good workability and rheological properties [4–6].

In order to maintain sufficient yield value and viscosity of fresh mix of SCC, and to reduce bleeding, segregation and settlement, the common practice is to use new generation high range water reducers, to limit the maximum coarse aggregate size and content, and to use low water powder ratios or use viscosity modifying admixtures. Therefore, one of the disadvantages of SCC is its cost, associated with the use of chemical admixtures and use of high volumes of Portland cement. High cement content usually introduces high hydration heat, high autogenous shrinkage and high cost. Moreover, the consumption of natural resources and carbon dioxide emissions associated with cement production can cause serious environmental impacts.

On the other hand, it is worldwide accepted that energy saving in building technology is one of the most important problems in the world. Reduction of energy usage can be taken place even by design methods [7,8] or using waste materials [9–11].

Nowadays, most industrial wastes are being used without taking full advantages of their characteristics or disposed rather than used. Among these materials, fly ash (FA), a by-product of thermal power plants, and ground granulated blast furnace slag (GGBFS) have been reported to improve the mechanical properties and durability of concrete when used as a cement replacement material [12,13]. It is worth mentioning that for example in Turkey, more than 13 million tons of FA has been produced per year, however, because of insufficient data on the properties of fly ash and concrete incorporating FA, only 5% of this amount is utilized in construction industry [14]. Therefore, one solution to reuse such industrial wastes and reduce the cost of SCC is the use of mineral admixtures such as limestone powder, natural pozzolans, GGBFS and FA.

The amount of FA in concrete for structural use is generally limited to 15–25% of the total cementitious materials. Concretes containing large amounts of FA were initially developed for mass concrete applications to reduce the heat of hydration [15]. Canada Centre for Mineral and Energy Technology first developed high volume FA concrete for structural use by the late 1980's [16]. In a study undertaken by Bouzoubaâ and Lachemi, it was shown that it was possible to design SCC with high volumes of FA by replacing up to 60% of cement with Class F FA [17]. Moreover, Nehdi et al. also studied the durability of SCC with high volume replacement materials (FA and ground granulated blast furnace slag), and concluded that SCC with 50% replacement with Portland cement of FA and slag can improve the workability and durability [18]. With this respect, it should be mentioned that a 50% replacement of each ton of Portland cement would result in a reduction of approximately 500,000 t of CO2. Using GGBFS or FA as a partial replacement takes advantage of the energy saving in Portland cement which is governed by AASHTO M302 [19].

According to Fava et al. [20], in SCCs with ground granulated blast furnace slag (GGBFS), strength increase can be achieved. Kulakowski et al. [21] reviewed the silica fume influence on reinforcement corrosion in concrete and the effect of metakaolin on transport properties of concrete were also investigated by Shekarchi et al. [22].

There are also some works on incorporating nanoparticles into concrete specimens to achieve improved physical and mechanical properties which most of them have focused on using SiO_2 nanoparticles in normal concrete [23], generally cement mortars and cement-based materials [24–26], self compacting concrete (SCC) [27] and high performance self compacting concrete (HPSCC) [4].

Production and application of HPSCC containing nanomaterials and mineral admixtures seems to be a promising and energy saving step toward sustainable construction and building technology. However, this would not be achieved without studying its performance before being widely adopted in construction. Also, the behavior of structural elements made with HPSCC needs better understanding, together with design provisions.

This paper investigates the effects of silica nanoparticles, silica fume and Class F fly ash on rheological, mechanical, thermal, transport and microstructural properties of HPSCC with different binder contents. The mechanical properties were assessed by compressive, splitting tensile and flexural strengths. Thermal properties were evaluated by thermogravimetric analysis and transport properties were evaluated by water absorption, capillary absorption and chloride ion penetration tests. The microstructure was also investigated through scanning electron microscopy (SEM) micrographs.

2. Materials

An ASTM Type II Portland cement (PC) was used to produce the various HPSCC mixtures. In addition, silica nanoparticles, silica fume and Class F fly ash were used as admixtures which are hereafter named as nano silica (NS), silica fume (SF) and fly ash (FA) respectively. Table 1 summarizes physical properties and chemical composition of the cement and silica fume. Scanning electron microscopy (SEM) of the silica nanoparticles is shown in Fig. 1 and the nanoparticles properties are presented in Table 2. Class F fly ash was used in this study which its physical and chemical properties are given in Table 3. SEM micrograph of Class F fly ash is also shown in Fig. 2. The coarse aggregate used was limestone gravel with a nominal maximum size of 12.5 mm. As fine aggregate, a mixture of silica aggregate sand and crushed limestone (as filler) was used with a maximum size of 4.75 mm. physical properties of the filler, fine and coarse aggregates are presented in Table 4. All aggregates in this research were used in dry form and the aggregates are a mixture of eight

Table 1
Chemical composition and physical properties of cement and silica fume.

Chemical analysis (%)	Cement	Silica fume
Sio_2	20<	93.6
Al_2O_3	6<	1.3
Fe_2O_3	6<	0.9
CaO	<50	0.5
MgO	<5	1
SO_3	<3	0.4
K_2O	<1	1.52
Na_2O	<1	0.45
Loss of ignition	<3	3.1
Specific gravity	3.15	2.2
Blaine fineness (cm^2/g)	3260	21090

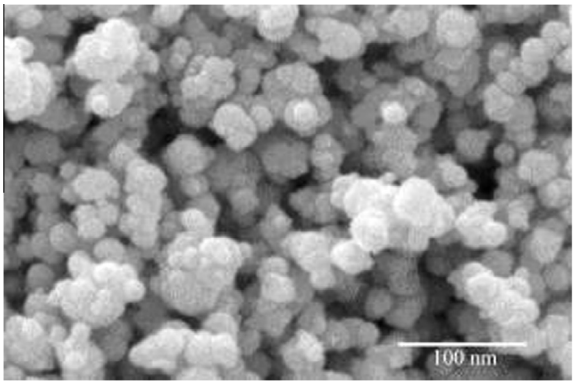

Fig. 1. SEM micrograph of silica nanoparticles.

Table 2
Properties of silica nanoparticles.

Diameter (nm)	Surface volume ratio (m^2/g)	Density (g/cm^3)	Purity (%)
15 ± 3	165 ± 17	<0.15	>99.9

Table 3
Chemical and physical properties fly ash.

Constituent	Percent by weight
Sio_2	52
Fe_2O_3	3.5
Al_2O_3	30
CaO	6.5
MgO	5
SO_3	1.6
Loss of ignition	3.7
Na_2O	0.58
K_2O	1.27
Color	Gray
Specific gravity	2.13

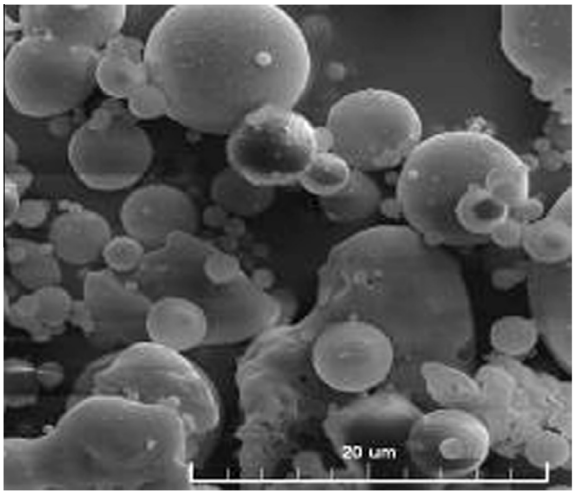

Fig. 2. SEM micrograph of Class F fly ash particles [6].

Table 4
Sieve analysis and physical properties of the filler, fine and coarse aggregates.

Sieve size (mm)	Filler (% passing)	Fine aggregate (% passing)	Coarse aggregate (% passing)
12.5	100	100	97.9
9.5	100	100	79.3
4.75	100	98.38	13.2
2.36	100	76.45	0
1.18	100	46.65	0
0.6	100	39.32	0
0.3	100	15.26	0
0.15	90.9	3.62	0
0.075	33.7	0	0
Bulk density (kg/m^3)		1460	1450
Specific gravity (g/m^3)		2.619	2.6
Absorption (%)	8	2.72	0.4

particle sizes of fine and coarse aggregates. A polycarboxylic-ether type superplasticizer (SP) with a specific gravity of between 1.06 and 1.08 was employed to achieve the desired workability in all concrete mixtures. Furthermore viscosity modifying agent (VMA) for better stability was used.

3. Grading

In fact, the packing theory of Fuller and Thompson [28] represents a special case of the more general packing equations derived by Andreasen and Andersen [29]. According to their theory, optimum packing can be achieved when the cumulative Particle Size Distribution (PSD) obeys Eq. (1) [30]:

$$P(D) = \left(\frac{D}{D_{max}}\right)^q \quad (1)$$

where P is the fraction that can pass through a sieve with opening diameter D; D_{max} is maximum particle size of the mix. The parameter q has a value between 0 and 1, Andreasen and Andersen [29] have found that optimum packing is obtained when $q = 0.37$. The grading by Fuller is obtained when $q = 0.5$ [30].

PSD curve of some of the mixtures used in this research has been compared with the Fuller and A&A optimized PSD curve, shown in Fig. 3. As shown, the more the PSD curve of the mixtures approaches the Fuller curve ($q = 0.5$), the more the results for the fresh HPSCC tests and segregation resistance of the mixes are improved. In this paper $q = 0.45$ was used and the modified grading curve is shown in Fig. 3. The figure shows four grading curves with three different values of q. Though $q = 0.37$ improves workability because of increase of finer grains, however it leads to strength and durability problems of the hardened concrete and hence it is not suitable to be used in high performance concrete mix design. Although strength improvement was expected by using Fuller grading curve, but it lead to decrease of finer grains compared to Andreasen and Andersen and resulted in segregation while making self-compacting concrete. In order to reach a more optimal gradation satisfying strength, durability and workability purposes, $q = 0.45$ was considered as a base and according to the available aggregates, it was tried to prepare a modified grading curve which is plotted in Fig. 3.

4. Mix proportions

A total number of 14 concrete mixtures were designed with a constant water/binder (w/b) ratio of 0.38 and total binder content of 400 and 500 kg/m^3. Concrete mixtures were prepared with 10%, 2% and 10% + 2% (by weight) replacement of Portland cement by SF, NS and blend of SF + NS respectively. Also some mixtures were designed with 5%, 10% and 15% replacement of Portland cement by FA. The mixture proportions of concrete and binder paste are given in Table 5. The abbreviations used in the study for labeling the mixtures were adopted in such a way that they clearly show the main parameters and their amount. HPSCC stands for high performance self compacting concrete which is followed by the binder content. NS, SF and FA denote nano silica, silica fume and fly ash respectively which are followed by their percentages.

5. Mixing procedure

Since the SP plays a very important role in the flowability of SCC mixes [31], a modified mixing procedure was adopted to take the benefit of action of adsorption of molecules of poly-carboxylic ether based SP on the cement particles for all the mixes. HPSCC mixtures were prepared by mixing the coarse aggregates, fine aggregates and powder materials (cement, nano silica, silica fume and fly ash) in a laboratory drum mixer. The powder material and aggregates were mixed in dry form for 2 min. Then half of the water containing the whole amount of Super plasticizer was poured and mixed for 3 min. After that, about 1 min rest was allowed and finally rest of the water containing VMA was added into the mixture and mixed for 1 min.

6. Preparation of the specimens

Cubic molds with dimensions of $150 \times 150 \times 150$ mm, $50 \times 50 \times 200$ mm and cylindrical molds with dimension of 100×200 mm were made for compressive, flexural and splitting tensile tests respectively. The molds for HPSCC were covered with polyethylene sheets and moistened for 48 h. Then the specimens were demolded and cured in water at a temperature of 20 °C until the test time. The compressive and splitting tensile strengths of the

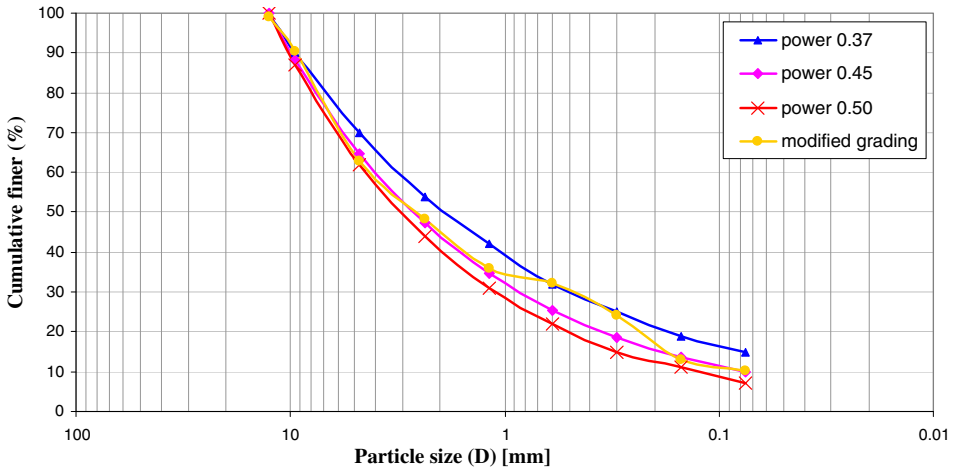

Fig. 3. Analysis of actual PSD of aggregates used with other models.

Table 5
Mix proportions of the concrete specimens.

No	Concrete ID	w/b	Cement	Silica fume	Nano silica	Fly ash	Filler	Fine aggregate	Coarse aggregate	Sp	VMA
			(kg/m^3)								
1	HPSCC400	0.38	400	–	–	–	177	1003	578	2.5	2
2	HPSCC500	0.38	500	–	–	–	177	1003	578	3.12	2.5
3	HPSCC400FA5%	0.38	380	–	–	20	177	1003	578	2.5	2
4	HPSCC400FA10%	0.38	360	–	–	40	177	1003	578	2.5	2
5	HPSCC400FA15%	0.38	340	–	–	60	177	1003	578	2.5	2
6	HPSCC500FA5%	0.38	475	–	–	25	177	1003	578	3.12	2.5
7	HPSCC500FA10%	0.38	450	–	–	50	177	1003	578	3.12	2.5
8	HPSCC500FA15%	0.38	425	–	–	75	177	1003	578	3.12	2.5
9	HPSCC400NS2%	0.38	392	–	8	–	177	1003	578	2.5	2
10	HPSCC400SF10%	0.38	360	40	–	–	177	1003	578	2.5	2
11	HPSCC400SF10NS2%	0.38	352	40	8	–	177	1003	578	2.5	2
12	HPSCC500NS2%	0.38	490	–	10	–	177	1003	578	3.12	2.5
13	HPSCC500SF10%	0.38	450	50	–	–	177	1003	578	3.12	2.5
14	HPSCC500SF10NS2%	0.38	440	50	10	–	177	1003	578	3.12	2.5

concrete samples were determined at 7, 28 and 90 days and the average of two trials was reported.

7. Testing of the specimens

When the mixing procedure was completed, tests were conducted on the fresh concrete to determine slump flow time, slump flow diameter and V-funnel flow time. Segregation was also visually checked during the slump flow test. From each concrete mixture, cubic samples of $150 \times 150 \times 150$ mm and $50 \times 50 \times 200$ mm, and cylinder samples of 100×200 mm were cast for the determination of compressive strength, flexural strength, split tensile strength respectively. Cubic samples of $100 \times 100 \times 100$ mm were also made for transport tests (water absorption, capillary absorption and chloride ion penetration tests). All specimens were cast in one layer without any compaction. At the age of 48 h, the specimens were demolded and stored in water at 21 ± 2 °C until the date of testing.

7.1. Tests on fresh concrete

The flow rate of a SCC mixture is influenced by its viscosity. When developing an SCC mixture in the laboratory, a relative measure of viscosity is useful. The time it takes for the outer edge of the concrete to spread and reach a diameter of 20 in. (500 mm) from the time the mold is first raised, based on the procedure described in the slump flow test, provides a relative measure of the unconfined flow rate of the concrete mixture. For similar materials, this time period, termed T50, gives an indication of the viscosity of the SCC mixture [32]. According to Nagataki and Fujiwara [33], the slump flow represents the mean diameter of the mass of concrete after release of a standard slump cone; the diameter is measured in two perpendicular directions. Basic workability requirements for an acceptable SCC are summarized by Khayat [34] as; excellent deformability, good stability, and lower risk of blockage.

Workability properties of SCC mixtures in this study were evaluated through the measurement of slump flow time (T50) to reach a concrete 50 cm spread circle, slump flow diameter (D) and V-funnel flow time according to the "Specification and Guidelines for SCC" prepared by EFNARC (European Federation for Specialist Construction Chemicals and Concrete Systems) [35].

7.2. Tests on hardened concrete

Tests performed on hardened concrete aimed to determine the mechanical properties including the compressive and splitting tensile strengths of the concrete specimens. Compressive strength values were measured according to BS-1881 [36] on $150 \times 150 \times 150$ mm cubes with two specimens for each concrete mix on 7, 28 and 90 days of curing.

The splitting tensile strengths were determined on 7, 28 and 90 days on cylinders measuring 100-mm diameter and 200 mm

height and cured in water until the date of test according the ASTM C496 [37]. Flexural tests were performed conforming to the ASTM C293 standard on 50 × 50 × 200 mm cubes [38]. Two specimens of each mixture were tested and the mean value was reported.

7.3. Thermogravimetric analysis test

Thermogravimetric analysis (TGA) test was conducted so that the weight loss of the concrete specimens due to heating can be determined. A Netzsch simultaneous thermal analyzer equipped with a Data Acquisition System was used for the tests. Specimens which were cured for 28 days were heated from 110 to 650 °C, at a heating rate of 4 °C/min and in an inert N2 atmosphere.

7.4. Transport tests

7.4.1. Absorption test

This test is based on BS 1881-Part 122 for testing water absorption in hardened concrete. The 100 × 100 × 100 mm specimens were dried in an oven at 45 °C for a week and after 14 days specimens reached to constant weight. The specimens were then immersed in water and scaled after 0.5, 1, 24, 72 and 168 h to check the weight increase and to calculate the water absorption percentage. In this test, water absorption can only take place in pores which are emptied during drying and filled with water during the immersion period.

7.4.2. Capillary test

When a non-saturated concrete element is in contact with water at one side and absorbed water evaporation is possible from the other side, a permanent flowing regime through capillary absorption is established [39]. The test carried out in this study for determination of capillary water absorption is based on RILEM CPC 11.2, TC 14-CPC for testing capillary absorption in hardened concrete. The 100 × 100 × 100 mm specimens were dried in the oven at 40 ± 5 °C. They were put on rods in a water bath in such a way that they were immersed in water for no more than 5 mm. In this test, unidirectional flow depths of the specimens were measured and results of capillary depths were reported.

7.4.3. Chloride ion penetration

After curing period of 90 days, 150 × 150 × 150 mm cubic specimens were immersed in 3% NaCl solution for 90 days. Then specimens were dried in the oven for 24 h. After that, in order to prepare some pulverized concrete samples (powder samples) for the test, all 6 faces of the cubic specimens were drilled by depths of 0–5, 5–10, 10–15, 15–20 and 20–30 mm and the concrete powder samples obtained from all 6 faces for each depth were blended and in this way, the samples were prepared for the next step of the test [ASTM C1218].

In this test method, total chloride content of pulverized concrete sample is determined by the potentiometric titration of chloride with silver nitrate [ASTM C114]. The pulverized concrete sample prepared is solved in nitric acid solution and then if the solution is acidic, a little of $NaHCO_3$ is added to this solution until pH value reaches 6 or 7. Then the K_2CrO_4 indicator is added so that the color of the solution changes to light yellow. Eventually, 0.05 N $AgNO_3$ is added until the color of the solution turns to orange-yellow (weak brown) and the volume of the $AgNO_3$ solution is measured. In order to determine the Cl ion percentage, the volume of the $AgNO_3$ solution is substituted in Eq. (2).

$$Cl^{-}(\%) = \frac{3.5453(V \cdot N)}{W} \quad (2)$$

W: weigh of pulverized (powder) concrete prepared from the sample, N: normality of $AgNO_3$ solution, V: volume of $AgNO_3$ solution.

8. Results and discussion

8.1. Rheological properties

In this experimental program, rheological properties of HPSCC was measured by slump flow (D (mm) and T50 (s)) and V-funnel. Table 6 lists the test results performed on fresh concrete. The slump flow diameters of all mixtures were in the range of 640–910 mm, slump flow times were less than 2.4 s, and the V-funnel flow times (s) were in the range of 2.5–12 s. The lowest V-funnel flow time as 2.5 s was measured for the HPSCC500FA10% and HPSCC500FA15%, while the HPSCC400SF10NS2% mixture had the highest flow time as 12 s. Incorporating SF and NS in binary and ternary systems, generally made the concretes more viscous. In order to increase V-funnel flow time of the concretes, the mineral admixtures as SF were used in binary blends. Almost all workability test results were in the range established by EFNARC [35] except some T50 flow times. T50 measurements of some mixtures were less than the lower limit; however, all concrete mixtures filled the molds by its own weight without the need for vibration. In addition to the above properties, visual inspection of fresh concrete did not indicate any segregation or considerable bleeding in any of the mixtures containing SF, NS, blended SF and NS, and FA during the slump flow and V funnel; however, a little bleeding was observed in the control specimens without any SF, NS and FA. The effect of including SF and NS with various volume fractions decreased flowability characteristics; however, they can improve the consistency of concrete mixtures. Less bleeding and segregation were also observed in the mixtures containing SF + NS.

Variations of slump flow (mm), T50 (s) and V funnel (s) are shown in Figs. 4–6 respectively. Nevertheless, the effect of FA with different percentages increased flowability characteristics and a little decreases the mix consistency. Generally it can be inferred from the figures that rheological properties of the mixtures containing 2% NS were close to those of the mixtures without admixtures and addition of 2% NS did not change the workability significantly. However, the rheological properties changed more in the mixtures containing 10% SF, 10% SF + 2% NS and different percentages of FA.

It has been found that addition of fine materials in the cement paste generally has a great effect on its viscosity. Limestone can improve the viscosity, and it is proved to be the best additive at 40% content [40]. On the other hand, silica fume and pozzolan do not seem to have the desired effects, meaning to lower the value of viscosity so as to have a more easy to flow paste [40].

Table 6
Rheological properties of HPSCC mixtures.

No	Concrete ID	Slump flow (mm)	T50 (s)	V funnel (s)
1	HPSCC400	750	2	9
2	HPSCC500	840	1.5	4
3	HPSCC400FA5%	760	2	8
4	HPSCC400FA10%	800	1.7	7
5	HPSCC400FA15%	830	1.5	6
6	HPSCC500FA5%	870	1.3	3.5
7	HPSCC500FA10%	890	1.1	2.5
8	HPSCC500FA15%	910	0.9	2.5
9	HPSCC400NS2%	740	2.1	10
10	HPSCC400SF10%	650	2.2	10
11	HPSCC400SF10NS2%	640	2.4	12
12	HPSCC500NS2%	820	1.7	4
13	HPSCC500SF10%	760	2.2	5
14	HPSCC500SF10NS2%	740	2.1	6
Acceptance criteria of SCC suggested by EFNARC		Slump flow		
		D (mm)	T50 (s)	
Min		650	2	6
Max		800	5	12

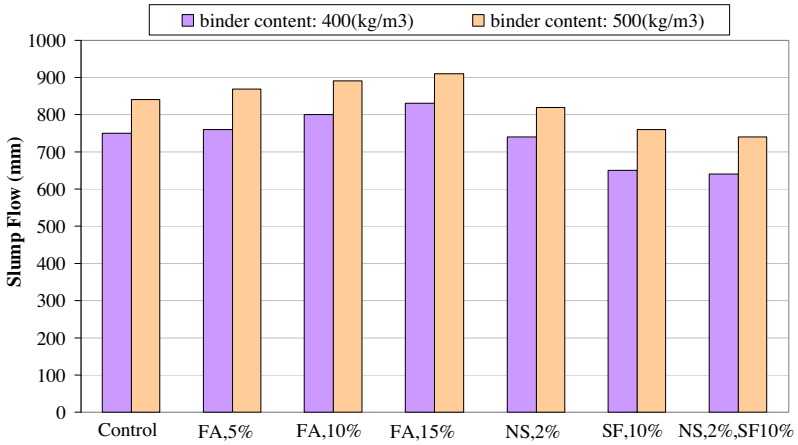

Fig. 4. Slump flow diameter changes for different mixes of HPSCC.

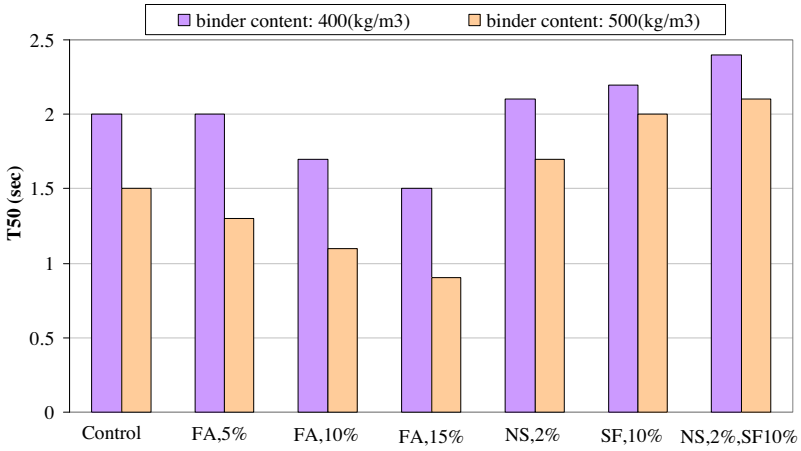

Fig. 5. T50 results for different mixes of HPSCC.

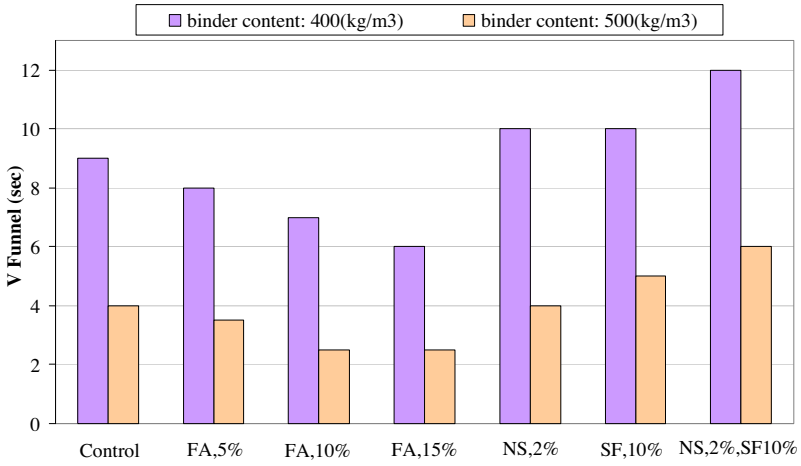

Fig. 6. V funnel flow time changes for different mixes of HPSCC.

The trends in Fig. 4 clearly reveal the increase of slump flow diameter by increasing the fly ash percentage from 0% to 15%. Binder content increase also has lead to increase of workability. The increase of slump flow diameter for 5%, 10% and 15% of fly ash is 10 and 80 mm, 10 and 70 mm, 30 and 70 mm for binder content of 400 and 500 respectively. This increase, from binder content of 400 to 500 kg/m^3 is 90 mm, 110 mm, 90 mm, 80 mm for 0%, 5%, 10% and 15% of fly ash respectively. In Fig. 5, an inverse trend compared to Fig. 4 can be seen i.e. T50 has been reduced by increasing the fly ash percentage and binder content. Addition of fly ash up to 15% reduced the T50 values from 2 s to 1.5 s, and 1.5 s to 0.9 s for binder content of 400 and 500 kg/m^3 respectively. Results of V funnel flow time of HPSCC are shown in Fig. 6. The figure obviously show that V funnel flow time decreases with the increase of fly

ash percentage and binder content which can be explained by ball bearing-shaped particles of Class F fly ash as shown in Fig. 2 and also increase of fine grains and water content (paste volume) in virtue of binder content increase which leads to workability enhancement. Addition of fly ash up to 15% reduced the $T_{v\text{-}f}$ values from 9 s to 6 s, and 4 s to 2.5 s for cement content of 400 and 500 kg/m^3 respectively.

Findings by other authors show that addition of lime stone and fly ash increase the slump flow of SCC and their combination lead to optimized consistency in terms of slump flow time and diameter [41]. Diamantonis et al. found that limestone is the best fine material that can be used as a fine additive, among fly ash, silica fume, and nano silica in their study. Based on their results, more improvement of cement paste rheological properties could be achieved by lime stone addition compared to other additives [40]. It has also been reported that incorporation of 2% NS by mass of cementitious materials reduced initial and final setting times by 90 and 100 min in high volume fly ash concrete. However, the setting times and early strength of these concretes were not affected by the silica fume significantly [42]. It was investigated that mortars with 3.5% nS and 3% SP show spread on table values higher than the ones with 20% SF and 0.7% SP [43].

8.2. Mechanical properties

Mechanical properties of HPSCC mixtures including the compressive, flexural and split tensile strength results are given in Table 7. This table presents the average of the compressive and flexural strengths as determined from two cubic specimens and splitting tensile strength as reported from two cylindrical specimens at each age. Increasing the SF content increased the compressive strength considerably, especially at older ages. Compared to control specimens, replacement by 10% SF in binary mixtures increased the compressive strength for binder content of 400 and 500 by 34, 9 and 9%, 9, 21 and 23% at, 7, 28 and 90 days respectively. Replacement by 2% NS in binary mixtures increased the compressive strength for binder content of 400 and 500 by 22%, 38% and 43%, 22%, 56% and 62% at 7, 28 and 90 days respectively. Replacement by 10% SF and 2% NS in ternary mixtures increased the compressive strength for binder content of 400 and 500 by 62%, 52% and 55%, 30%, 67% and 73% at 7, 28 and 90 days respectively. Generally in binary mixtures, the compressive strength improvement was higher in the mixtures containing 2% NS and the highest in ternary mixtures. Generally in all ages (7, 28 and 90 days) ascending trends were observed in compressive strength values by increasing the binder content.

With the increase in fly ash content from 0% to 15%, HPSCC mixes showed loss of compressive strengths at 7 and 28 days but at 90 day age compressive strength was developed. The compressive strength increased with a decrease in the percentage of the fly ash at low ages and increase of binder content.

To make the results more illustrative, compressive strength results for HPSCC at 10% level of cement replacement by SF, 2% replacement by NS, ternary blends of 10% SF and 2% NS, and 0–15% replacement by FA compared to control samples at 7, 28 and 90 days are shown in Fig. 7. It can be noted from the results that in 28-day old specimens and for 5%, 10% and 15% of fly ash, compressive strength losses of "22%, 28% and 34%", "17.9%, 23.2% and 31.2%" were observed for binder content of 400 and 500 kg/m^3 respectively. However, in the 90-day old specimens and for binder content of 400 kg/m^3, strength decrease of 5.2% and 1% and increase of 3.5% was observed for 5%, 10% and 15% of fly ash respectively. For binder content of 500 kg/m^3, strength decrease of 0.3% and increase of 5.8% and 7% was also observed for 5%, 10% and 15% of fly ash respectively.

Many researchers have investigated compressive strength of SCC containing different admixtures. Wongkeo et al. found that FA addition decreases compressive strength while SF at 5 and 10 wt% increases compressive strength of SCC. The reduction due to FA is attributed to its slow pozzolanic reaction and the dilution effect [44]. It was reported that incorporation of 2% NS by mass of cementitious materials increased 3- and 7-day compressive strengths of high-volume fly ash concrete by 30% and 25%, respectively, in comparison to the reference concrete with 50% fly ash. Similar trends were observed in high-volume slag concrete [42]. Behfarnia et al. found that replacement of cement content with nano-SiO2 improved the compressive strength of concrete mixes used in this research. In their study, the optimum content of nano-SiO2 in concrete in order to increase its compressive strength was 5 wt% [45]. A review on nanotechnology in concrete reported a comparison of nanoparticles' effect on compressive strength of cement mortars for nano-SiO_2 (NS), nano-Fe_2O_3 (NF) and silica fume at 7 and 28 days [46]. The highest values were obtained at NS-10% and NF-3%.

Regarding splitting tensile strength, it can be inferred from the results that the highest values belong to the mixtures containing both NS and SF with binder content of 500 kg/m^3. Compared to control specimens, replacement by 10% SF and 2% NS in ternary mixtures increased the splitting tensile strength for binder content of 400and 500 by 17%, 33% and 25%, and 27%, 2% and 11% at 7, 28 and 90 days respectively. In the same mixtures, binder content increase has also lead to average increase of splitting tensile strength by about 4%. In general, it may be seen from the results

Table 7
Mechanical properties of HPSCC mixtures.

No	Concrete ID	Compressive strength (MPa)			Splitting tensile strength (MPa)			Flexural strength (MPa)		
		7 days	28 days	90 days	7 days	28 days	90 days	7 days	28 days	90 days
1	HPSCC400	36.4	51.8	53.1	2.9	3.6	3.9	3.4	3.9	5.3
2	HPSCC500	40.2	52.5	53.2	3.7	4.7	4.8	4	4.8	5.9
3	HPSCC400FA5%	32.7	40.4	50.3	2.1	2.9	3.7	3.3	3.7	5.3
4	HPSCC400FA10%	26.9	37.3	52.5	2.1	2.6	3.8	3	3.7	5.2
5	HPSCC400FA15%	22.4	34.2	55	2.1	2.4	3.7	2.9	3.6	5.4
6	HPSCC500FA5%	33.2	43.1	53	2.5	3	4.6	4	4.6	6
7	HPSCC500FA10%	31.5	40.3	56.3	2.1	2.8	4.7	3.8	4.5	6.1
8	HPSCC500FA15%	30.1	36.1	60.2	2.3	2.7	4.8	3.7	4.5	6.2
9	HPSCC400NS2%	44.3	71.3	75.9	3	3.7	4.4	4.2	5.7	6.4
10	HPSCC400SF10%	48.7	56.5	58.1	3.1	3.7	4.3	3.8	4.6	5.9
11	HPSCC400SF10NS2%	59	78.8	82.4	3.4	4.8	4.9	4.2	6.2	7.8
12	HPSCC500NS2%	49.1	82.1	86.1	3.6	4.7	4.9	4.6	6.1	7.2
13	HPSCC500SF10%	43.9	63.4	65.1	3.7	4.7	4.8	4.3	5.2	6.3
14	HPSCC500SF10NS2%	52.3	87.9	92.1	3.7	4.8	5.3	4.8	7.3	9

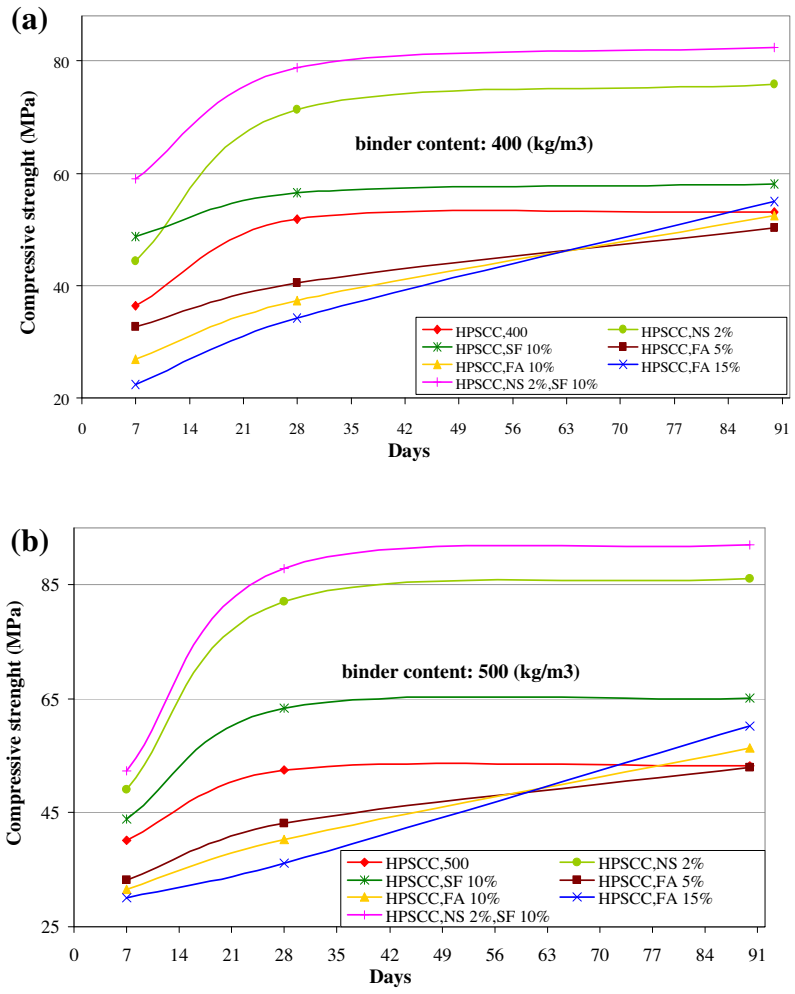

Fig. 7. Compressive strength results of HPSCC mixtures with binder content of (a) 400 kg/m^3, (b) 500 kg/m^3.

that the splitting tensile strength has increased significantly by addition of both NS and SF. It is also noted that the splitting tensile strength has increased rather significantly at more advanced ages.

Splitting tensile strength generally increased with a decrease in the percentage of the fly ash and an increase in binder content. At the age of 28 days, addition of fly ash from 0% to 15% reduced the split tensile strength from 3.6 to 2.4, and 4.7 to 2.7 MPa for binder content of 400 and 500 kg/m^3 respectively. However at the age of 90 days, the split tensile strength changes for 0–15% of fly ash were from 3.9 to 3.7, and 4.8 to 4.8 MPa for binder content of 400and 500 kg/m^3 respectively.

Similar trends were found by others. Nazari et al. found that addition of GGBFS content up to 45 wt% results in increased split tensile strength and SiO2 nanoparticles incorporation up to 3 wt%, could also have beneficial effect [27]. Jalal et al. in another study reported enhanced split tensile strength of SCC by addition of nano-TiO2 up to 4 wt% [5].

Flexural strength results of different HPSCC mixtures are plotted in Fig. 8 for different binder contents. Compared to control specimens, replacement by 10% SF + 2% NS in ternary mixtures increased the flexural strength for binder content of 400 and 500 by 23.5%, 58.9% and 47%, and 20%, 52% and 52% at 7, 28 and 90 days respectively. Replacement by 15% FA in the mixtures increased the flexural strength for binder content of 400 and 500 by 1.8% and 5% at 90 days respectively. However at earlier ages, the flexural strengths decreased by increasing the FA contents.

The use of CNF to 0.08%VF in the pastes specimens has been reported to increase the flexural strength by 30%. However, early age surface cracking also increased. The reduction in the size particle of the silica addition accelerated material stiffening and increased cracking risk [47].

According to Yu et al., the addition of waste bottom ash (WBA) reduces the compressive strength of the designed concrete. However, due to the coarse surface of WBA and the thread-like stuff on its surface, the flexural strength of the designed concrete can be slightly enhanced. After the nano-silica and hybrid fibers are added into the concrete, its mechanical properties (especially the flexural strength) can be significantly improved [48]. Beigi et al. found that increasing nanosilica content to 4 wt.%, increases the tensile and flexural strengths more significantly which is because of the filling and pozzolanic effects of nanosilica in contact area between fibers and cement matrix [49].

Several studies have been conducted on flexural strength of cementitious composites reinforced by Silica nano-particles and some possible reasons have been represented to show the increment of flexural strength:

1. When a small amount of the nano-particles is uniformly dispersed in the cement paste, the nano-particles act as a nucleus to tightly bond with cement hydrate and further promote cement hydration due to their high activity, which is favorable for the strength of cement mortar [50,51].

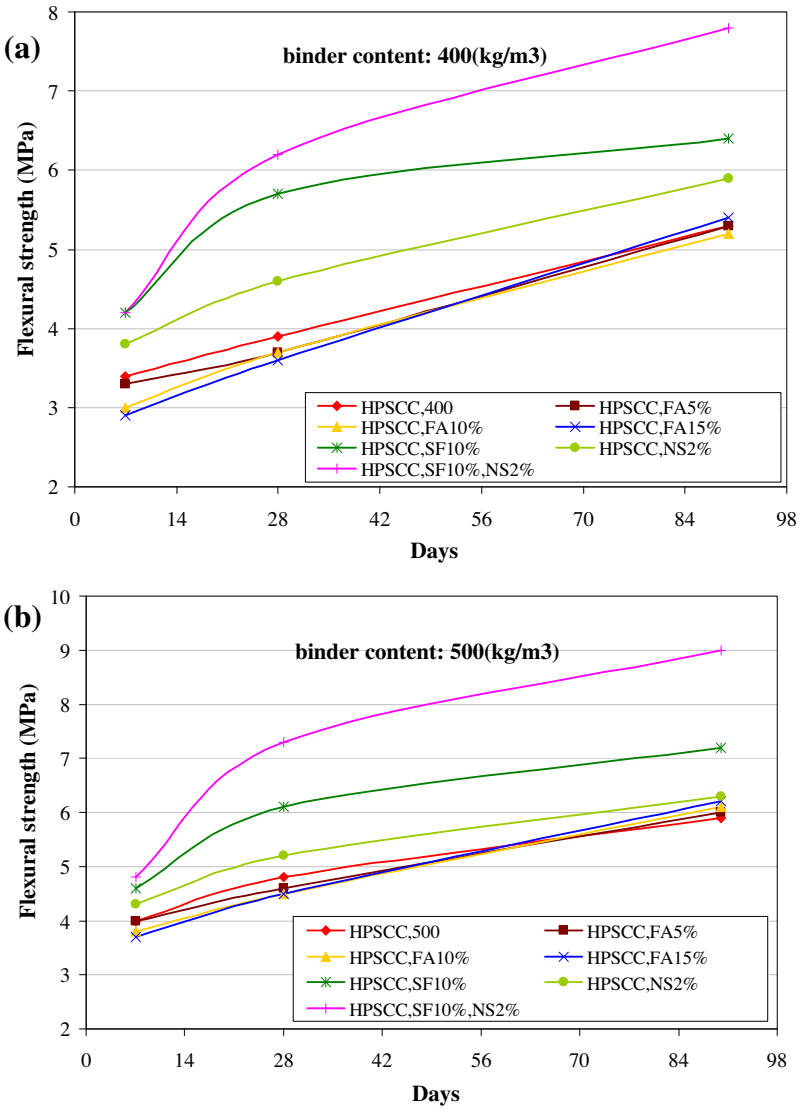

Fig. 8. Flexural strength results of HPSCC mixtures with binder content of (a) 400 kg/m^3, (b) 500 kg/m^3.

2. The nano-particles among the hydrate products will prevent crystals from growing which are positive for the strength of cement paste [51–53].
3. The nano-particles fill the cement pores, thus increasing the strength. Nano-SiO_2 can contribute in the hydration process to generate C–S–H through reaction with $Ca(OH)_2$ [54,55].

8.3. TGA results

Table 8 shows the thermogravimetric analysis results of different HPSCC specimens measured in the 110–650 °C range in which dehydration of the hydrated products occurred. The results show that after 28 days of curing, the loss in weight of the specimens is increased by decreasing the PC content in concretes. The results also showed that the loss in weight of the specimens is increased by increasing NS and SF in concrete mixtures. Increasing the FA percentage in the binder resulted in weight loss increase, however the weight losses were not as significant as those occurred in the specimens containing NS and SF. The most noticeable weight losses belonged to the mixtures containing 10%SF + 2%NS with binder content of 500 kg/m^3. The increase in weight loss could be due to more formation of CH and C_3H compounds in the cement paste. Furthermore, more rapid formation of hydrated products in presence of silica nanoparticles and silica fume could be the reason of more weight loss.

Table 8
Thermogravimetric analysis results of HPSCC specimens.

No	ID	Weight loss in the range of 110–650 °C (%)
1	HPSCC400	13.5
2	HPSCC500	14.5
3	HPSCC400FA5%	14.2
4	HPSCC400FA10%	14.9
5	HPSCC400F15%	15.6
6	HPSCC500FA5%	14.8
7	HPSCC500FA10%	15.9
8	HPSCC500FA15%	16.3
9	HPSCC400NS2%	17.8
10	HPSCC400SF10%	18.1
11	HPSCC400SF10NS2%	19.3
12	HPSCC500NS2%	18.8
13	HPSCC500SF10%	19.2
14	HPSCC500SF10NS2%	19.9

8.4. Transport properties

8.4.1. Water sorption

The water absorption results of the concrete samples at different time intervals are presented in Table 9. As can be seen, increase in binder content from 400 to 500 kg/m^3 resulted in water absorption decrease by 15.3% respectively at the first time step of water absorption (0.5 h) in the samples without any admixtures. Water absorption decrease in the samples containing 2% NS in the first time step appeared to be 35% and 32% for binder content of 400 and 500 respectively. Addition of 10% SF resulted in water absorption decreases in the same duration by 31% and 34% for binder content of 400 and 500 respectively, which is similar to the values obtained in the mixtures containing 2% NS. The reductions in water absorption in the mixtures containing 2% NS + 10% SF were obtained as 46% and 50% for binder content of 400 and 500 respectively, which is noticeable and reveals the good performance of SF + NS blends in the HPSCC mixtures.

Water absorption decrease in the samples containing 5% of fly ash in the first time step appeared to be 4% and 9% for binder content of 400 and 500 respectively. The reductions for fly ash addition by 10% and 15% were 19%, 18% and 27%, 27% for similar binder contents respectively. Considering the results, the enhanced water resistant performance of the concrete samples containing fly ash may be inferred.

The water permeability test carried out by Ji et al. shows that the nano-SiO_2 concrete has better water permeability resistant behavior than the normal concrete [56]. In another study, Mortars with 7% NS, exhibited the highest values of water absorption and apparent porosity (between samples with 0.35 W/B), while these values decreased for mortars with 20% SF [43]. Wongkeo et al. study revealed that water absorption has a direct relationship with the voids so the absorption decreased as the voids decreased. Thus, at the same w/b ratio, the water absorption of all SCC containing FA was higher than Portland cement control and tends to decrease with increasing SF content [44].

The results generally show desirable effect of FA as a natural pozzolan on water absorption properties of the concrete samples. With this respect, more desirable performances were observed in the mixtures with binder content and FA percent of 500 kg/m^3, 15% FA. Although water absorption decreases were also observed in the mixtures containing lower percentages of FA, however the values were not significant.

8.4.2. Capillary water absorption

The capillary water absorption results of the HPSCC samples at different time intervals are presented in Table 10. The results show that the height of absorbed water in the concrete samples has decreased by increasing the binder content from 400 to 500 and addition of NS, SF and FA admixtures. Increase in binder content from 400 to 500 lead to capillary water absorption from 2.8 to 2.5 mm during three hours and from 8.6 to 6.6 mm during 72 h respectively, which the capillary water height decreases seem more significant at longer times. It may be due to the fact that the samples fully dried in the oven have more tendency to absorb water at earlier times, however at longer times the effect of binder content, NS, SF and especially FA admixtures comes to be revealed more and the results considered to be more realistic and reliable. Addition of 2% NS resulted in capillary water absorption of 3.6 and 3 mm for binder content of 400 and 500 respectively during 72 h for which the reductions of 58% and 54% compared to the mixtures without any admixture can be considered. Addition of 10% SF with binder content of 400 and 500 resulted in capillary water absorption decrease by 60% and 53% respectively during 72 h compared to the mixtures without any admixture. The same reductions observed for mixtures containing blend of 2% NS + 10% SF were 66% and 66% respectively. As can be seen, the water proofing effects of SF and NS on HPSCC tend to appear more obviously in the mixtures containing both SF and NS with higher binder content. As can be inferred from the water absorption results, this performance may be attributed to the more packed and refined microstructure and pore structure of the concrete achieved by addition of SF + NS.

Addition of 5% fly ash resulted in capillary water absorption of 8.3 and 6.3 mm for cement content of 400, 450 and 500 respectively during 72 h for which the reductions of 3.5% and 4.7% compared to the mixtures without any pozzolan can be considered. By increasing the fly ash percentage more significant results were recognized. Addition of 10% and 15% FA with binder content of 400 and 500 resulted in capillary water absorption decrease by 27% and 12% and 44% and 42.5% respectively during 72 h compared to the mixtures without any FA. As can be seen, the water proofing effects of fly ash on high performance self compacting concrete tend to be revealed more obviously at higher percentages of FA addition. As observed in water absorption results, this performance may be attributed to the more packed microstructure and pore structure of the concrete by addition of fly ash. At the nano scale, the results demonstrated that the chloride penetration velocities were more closely related to the change in the CPDs in the cement matrix than to the APDs, including the capillary pores, in both the ITZ and the cement matrix as detected by the MIP [41].

8.4.3. Chloride ion penetration

In this test, the chloride ion penetration has been determined as a fraction of the concrete sample weight. Presented in Table 11 are the results of chloride percentage at different depths of the

Table 9
Results of water absorption by time.

No	Concrete ID	Water absorption (%) Time (h)					
		0.5 h	1 h	24 h	48 h	72 h	168 h
1	HPSCC400	2.6	3.2	5.3	5.5	5.6	5.8
2	HPSCC500	2.2	3.1	4.3	4.4	4.6	4.9
3	HPSCC400FA5%	2.5	3	5.1	5.2	5.4	5.6
4	HPSCC400FA10%	2.1	2.2	3	3.4	3.6	3.9
5	HPSCC400F15%	1.9	2.1	2.5	2.9	3	3.3
6	HPSCC500FA5%	2	2.9	3.9	4	4.2	4.3
7	HPSCC500FA10%	1.8	1.9	2.5	2.7	2.8	3.1
8	HPSCC500FA15%	1.6	1.9	2.3	2.5	2.6	2.8
9	HPSCC400NS2%	1.7	2.2	2.7	2.8	2.85	3
10	HPSCC400SF10%	1.8	2.25	2.65	2.7	2.74	3
11	HPSCC400SF10NS2%	1.4	1.8	2	2.2	2.3	2.4
12	HPSCC500NS2%	1.5	1.95	2.4	2.5	2.6	2.7
13	HPSCC500SF10%	1.44	1.7	2.2	2.3	2.4	2.5
14	HPSCC500SF10NS2%	1.1	1.4	1.6	1.7	1.9	2

Table 10
Results of capillary absorption by time.

No	Concrete ID	Capillary water absorption (mm) Time (h)			
		3	6	24	72
1	HPSCC400	2.8	2.82	6.5	8.6
2	HPSCC500	2.5	3.4	5.5	6.6
3	HPSCC400FA5%	2.7	3.7	6.2	8.3
4	HPSCC400FA10%	2.4	3.2	5	6.3
5	HPSCC400F15%	2	2.9	4.3	5.8
6	HPSCC500FA5%	2.4	3.2	5.3	6.3
7	HPSCC500FA10%	2	2.9	4.3	5.8
8	HPSCC500FA15%	1.9	2.4	3.3	3.8
9	HPSCC400NS2%	2.2	2.7	3.4	3.6
10	HPSCC400SF10%	2.1	2.5	3.3	3.4
11	HPSCC400SF10NS2%	1.9	2	2.8	2.9
12	HPSCC500NS2%	1.8	2.3	2.9	3
13	HPSCC500SF10%	1.7	2.16	2.9	3.1
14	HPSCC500SF10NS2%	1.5	1.7	2.1	2.2

Table 11
Chloride ion percentage at different average depths of the concrete samples.

No	Concrete ID	Chloride ion percentage (%) Mean of depth (mm)				
		2.5 (mm)	7.5 (mm)	12.5 (mm)	17.5 (mm)	25 (mm)
1	HPSCC400	4.2	1.7	0.8	0.52	0.19
2	HPSCC500	2.98	1.4	0.65	0.37	0.14
3	HPSCC400FA5%	4	1.5	0.7	0.48	0.18
4	HPSCC400FA10%	3.5	1.3	0.65	0.43	0.16
5	HPSCC400F15%	3.2	1.1	0.62	0.4	0.15
6	HPSCC500FA5%	2.7	1.3	0.58	0.35	0.13
7	HPSCC500FA10%	2.4	1.15	0.54	0.32	0.12
8	HPSCC500FA15%	2.3	0.9	0.43	0.31	0.1
9	HPSCC400NS2%	2.4	1.1	0.62	0.42	0.15
10	HPSCC400SF10%	2.3	0.81	0.51	0.32	0.14
11	HPSCC400SF10NS2%	1.6	1	0.4	0.29	0.09
12	HPSCC500NS2%	2	0.85	0.43	0.32	0.12
13	HPSCC500SF10%	1.7	0.4	0.43	0.23	0.09
14	HPSCC500SF10NS2%	1.3	0.55	0.33	0.11	0.03

concrete samples. The results show a general decrease in chloride percentage by depth of concrete sample which conveys the fact that the concrete ingredients especially aggregates are clear from chloride ions. In depth of 0–5 mm, increase in binder content from 400 to 500 in the samples without any admixture resulted in reductions of chloride ion amount by 29%. In depth of 0–5 mm of the samples containing 2% NS, chloride ion penetration decreased by 43% and 43% for binder contents of 400 and 500 respectively. The reductions in the samples containing 10% SF were obtained as 52% and 43% for the same binder contents respectively. The samples containing blend of 10% SF + 2% NS showed significant chloride ion penetration decrease as 62% and 56% for the same binder contents respectively.

In depth of 0–5 mm of the samples containing 5% FA, chloride ion penetration decreased by 5% and 9.3% for binder contents of 400 and 500 respectively. The reductions in the samples containing 10% and 15% FA were observed as 16.6%, 19.4% and 24%, 23% for binder contents of 400 and 500 respectively.

As can be considered, SF and NS addition has resulted in relatively significant decrease in chloride ion percentage which may be in virtue of more refined pore structure of the concrete obtained by addition of the admixtures especially nanoparticles and pozzolanic effect of this material.

The results of chloride ion percentage versus average depth of the concrete sample for different binder contents and admixtures amount are plotted in Fig. 9. The curves obviously show

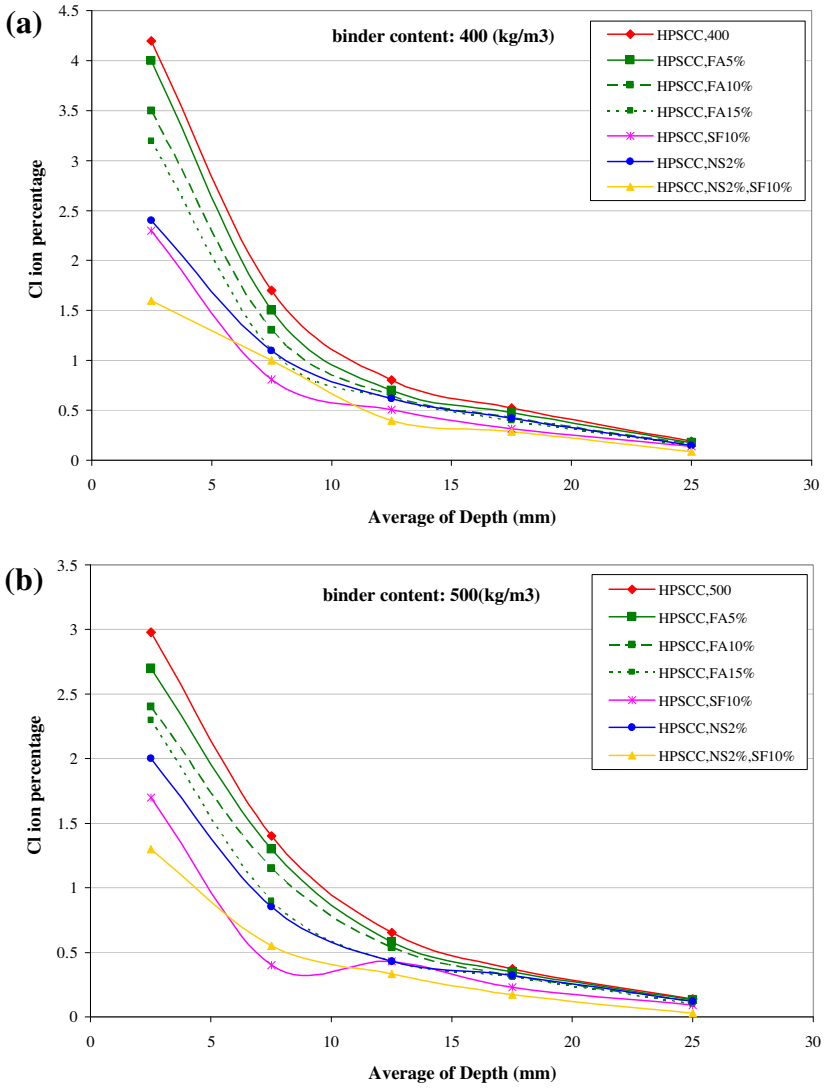

Fig. 9. Chloride ion percentage results of HPSCC mixtures with binder content of (a) 400 kg/m^3, (b) 500 kg/m^3.

descending trends by increase in depth. Comparison is easier in lower depths, however in higher depths the curves get closer together and the differences get smaller. According to this figure, again it is confirmed that the mixture with binder content of 500 containing NS + SF has the most desirable durability performance.

Comparable results were obtained by some researchers. The work done by Wongkeo et al. shows that at the same w/b ratio, the charges passed of Portland cement control concrete were higher than that of FA and SF concretes. Furthermore, the charges passed of FA concrete were higher than that of SF concrete [44]. Another study demonstrates that the use of lime stone (LP) at relatively high replacement of cement increased the chloride penetration velocity of LP–SCC as compared with both the use of cement only (without any replacement) and the incorporating of mineral admixture such as FA and FA + SF at the same replacement percentage [41]. Results of water absorption and catalyzed chloride ion penetration tests show that nanosilica has a great influence on the reduction of water absorption and chloride ion penetration into fiber-reinforced concrete [49].

8.5. Microstructures

The microstructure of the HPSCC containing Class F fly ash as investigated by Scanning Electron Microscopy (SEM) at different ages is shown in Fig. 10. The mechanical, rheological and durability properties are influenced by the microstructure and might be explained by the SEM micrographs. As can be seen in Fig. 10-1-a, the ball bearing-shaped particles of Class F fly ash are distributed in the HPSCC paste and they could facilitate the flowability of the paste and therefore improve the workability and rheological properties of the mixture. However, in higher ages the reactions in the HPSCC paste evolve and by formation of more reaction products, a denser microstructure may be expected as shown in Fig. 10-1-b. At more advanced ages, the pozzolanic effects of fly ash and the reactions in the composite paste rather reach to the highest level and the reaction products appear crystalline in the microstructure and even denser pore structure may be reached as appeared in Fig. 10-1-c. The development of the compressive strength at higher ages might be explained by this evolutionary trend of the pore

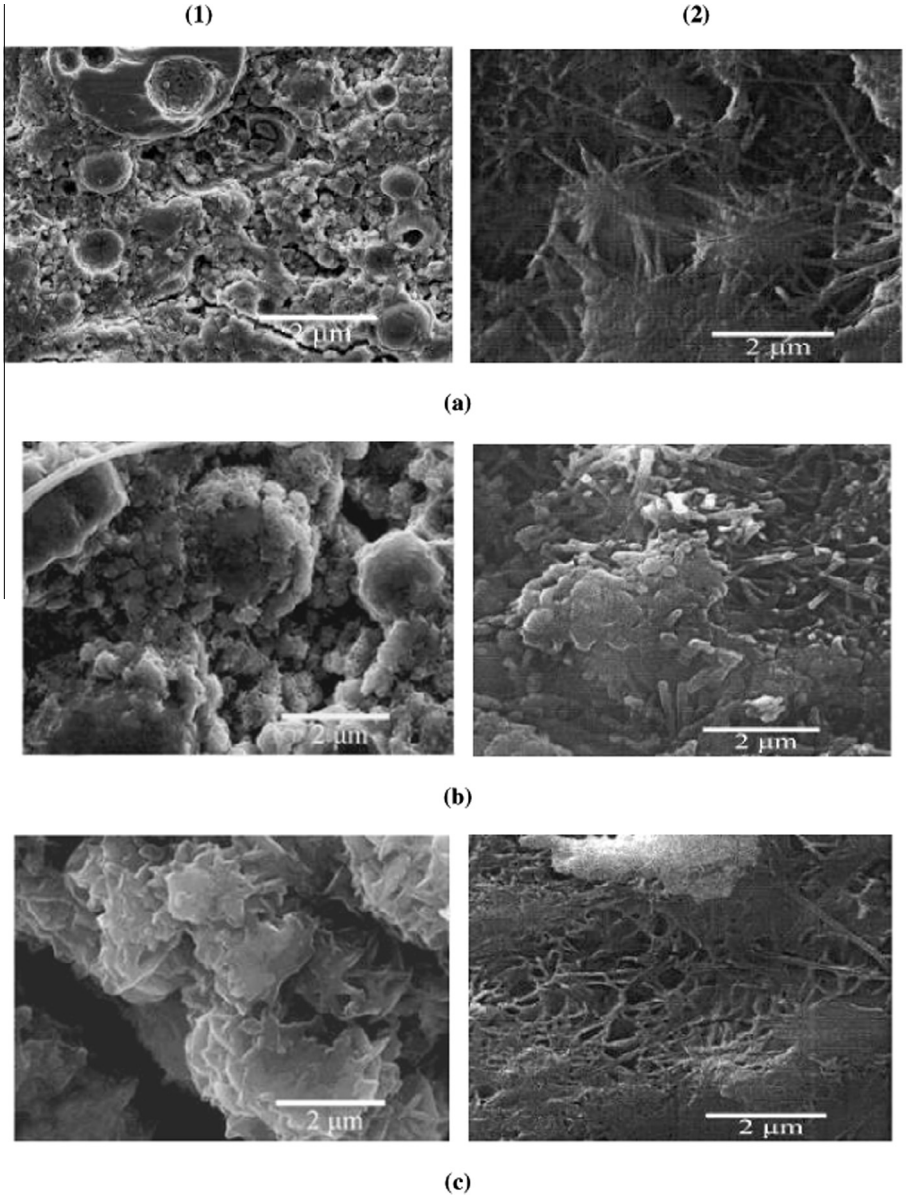

Fig. 10. SEM micrographs of HPSCC mixtures (1) with 15% fly ash and (2) without fly ash at 7 days (series a), 28 days (series b) and 90 days (series c) [6].

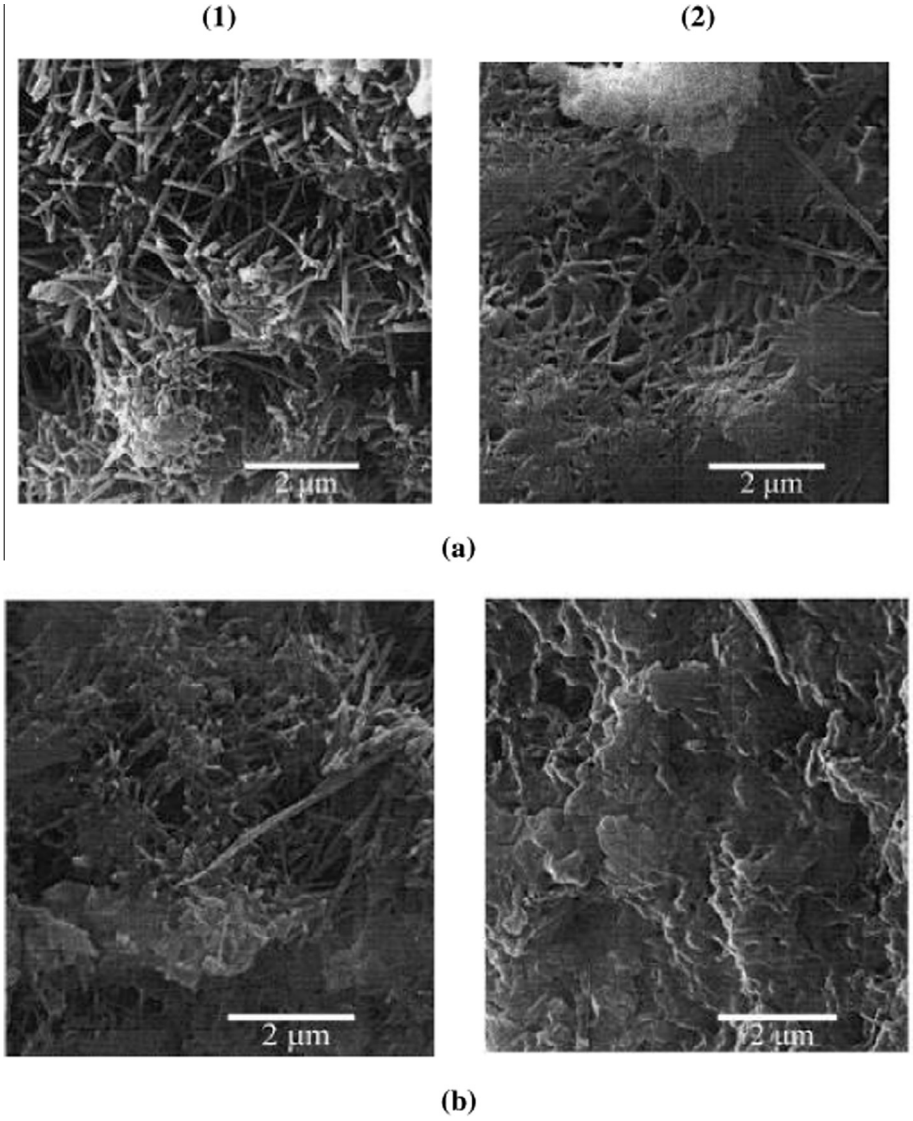

Fig. 11. SEM micrographs of HPSCC mixtures (a) without admixtures, (b) with 10% SF, (c) with 2% NS and (d) with 10% SF + 2% NS at 7 days (series 1) and 90 days (series 2) [4].

structure. Regarding durability properties, it may be deduced from the micrographs that the pore structure of the mixtures containing fly ash get denser and more packed especially at more advanced ages and the pores get smaller and it can result in less water absorption, capillary absorption and Cl ion penetration and more resistivity. Regarding microstructure effect on transport properties, Beigi et al. mentioned that reduction in chloride ion penetration is because of high activity of nanosilica that facilitates reaction between nanosilica and calcium hydroxide (with low resistance against chemical attacks) that compacts it to calcium silicate hydrate [49]. This compaction could improve and strengthen microstructure of concrete against chloride ion penetration [49]. Diamantonis et al. concluded that there is a synergy between limestone and fly ash that results in a denser micro-structure, due to better filling the void space among the granules [40]. Better durability of nano-SiO_2 blended concrete was also attributed to the fact that the nano-SiO_2 particles can fill the voids of the C–S–H gel structure and act as nucleus to tightly bond with C–S–H gel particles, making binding paste matrix denser, and long-term mechanical properties and durability of concrete are expected to be increased [56]. It was also maintained that the chloride migration coefficient is proportional to both the thickness and the porosity of the ITZ. High ITZ thickness can increased the capillary pore's percolation in the ITZ and thus ITZ thickness was more responsible than ITZ porosity alone in determining the chloride ingress [41].

The mechanism that the nano particles improve the pore structure of concrete can be interpreted as follows [27]: suppose that nano particles are uniformly dispersed in concrete and each particle is contained in a cube pattern, therefore the distance between nano particles can be determined. After the hydration begins, hydrate products diffuse and envelop nano particles as kernel [27]. If the content of nano particles and the distance between them are appropriate, the crystallization will be controlled to be a suitable state through restricting the growth of $Ca(OH)_2$ crystal by nano particles. Moreover, the nano particles located in cement paste as kernel can further promote cement hydration due to their high activity. This makes the cement matrix more homogeneous and compact. Consequently, the pore structure of concrete is improved evidently such as the concrete containing nano-SiO_2 in the amount of 1% by weight of binder [27].

On the whole, the addition of silica fume and especially silica nanoparticles improves the pore structure of concrete. On the one hand, nano particles can act as a filler to enhance the density of concrete, which leads to the porosity of concrete reduced

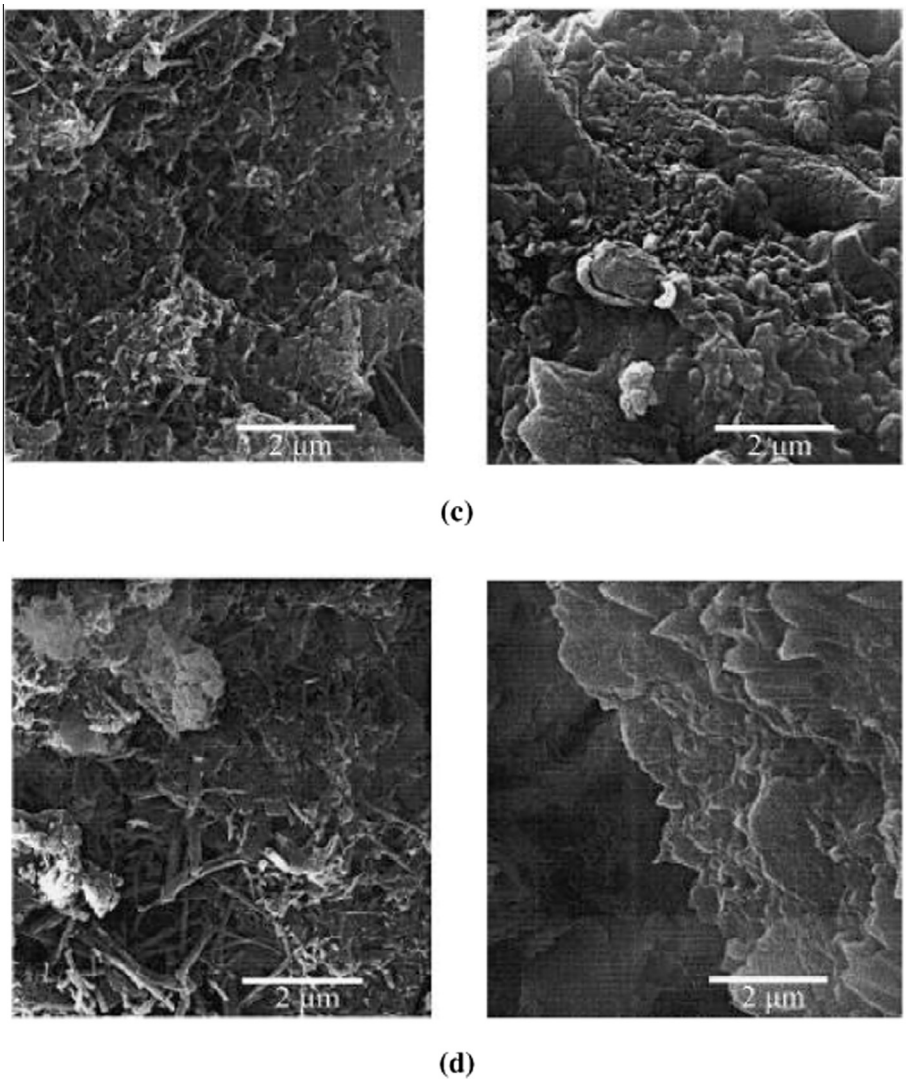

Fig. 11 (*continued*)

significantly. On the other hand, nano particles can not only act as an activator to accelerate cement hydration due to their high activity, but also act as a kernel in cement paste which makes the size of $Ca(OH)_2$ crystal smaller and the tropism more stochastic. Some researchers explain that nano-SiO_2 can absorb the $Ca(OH)_2$ crystals, and reduce the size and amount of the $Ca(OH)_2$ crystals, thus making the interfacial transition zone (ITZ) of aggregates and binding paste matrix denser [56]. Others found that the modification in the chemistry of the ITZ due to the use of different fillers and mineral admixture as a high partial replacement leads to different ITZ porosities which was more noticeable in the case of using the FA + SF replacement [41]. Yu et al. concluded that the simultaneous addition of nanosilica and hybrid fibers into UHPFRC can effectively restrict and minimize the cracks leading to significant enhancement of mechanical properties of the designed UHPFRC with waste bottom ash (WBA) [48].

The high enhancement of compressive strength and splitting tensile strength in the SF and NS blended HPSCC is due to the rapid consuming of $Ca(OH)_2$ which was formed during hydration of Portland cement specially at early ages related to the high reactivity of NS particles. As a consequence, the hydration of cement is accelerated and larger volumes of reaction products are formed. Also NS particles recover the particle packing density of the blended cement, directing to a reduced volume of larger pores in the cement paste. Fig. 11a–d show respectively the scanning electron micrographs (SEM) of HPSCC without admixture, with 10% SF, with 2% NS, and blend of 10% SF and 2% NS after 7 days (Fig. 11, series 1) and 90 days (Fig. 11, series 2) of curing in water. C–S–H gel which is existed in isolation is enclosed by some of needle-hydrates in the SEM of cement paste (Fig. 11a). On the other hand, the micrograph of the mixture containing SF (Fig. 11b) and especially NS (Fig. 11c and d) revealed a compact formation of hydration products and a reduced content of $Ca(OH)_2$ crystals. Fig. 11c and d show a more compact mixture after all days of curing which indicate rapid formation of C–S–H gel in presence of Silica nano particles.

References

[1] ACI Committee 363 RState-of-the-art Report on High-Strength Concrete, American Concrete Institute, Farmington Hills, USA, 1997.
[2] H. Okamura, M. Ouchi, Self-compacting concrete, J. Adv. Concr. Technol. 1 (2003) 5–15.
[3] M. Sahmaran, A. Yurtseven, I.O. Yaman, Workability of hybrid fiber reinforced self-compacting concrete, J. Build. Environ. 40 (2005) 1672–1677.
[4] M. Jalal, E. Mansouri, M. Sharifipour, A.R. Pouladkhan, Mechanical, rheological, durability and microstructural properties of high performance self compacting concrete containing SiO_2 micro and nanoparticles, 2011, doi: 10.1016/j.matdes.08.037.

[5] M. Jalal, A.A. Ramezanianpour, M. Khazaei Pool, Split tensile strength of binary blended self compacting concrete containing low volume fly ash and TiO_2 nanoparticles, Composites B 55 (2013) 324–337.
[6] M. Jalal, M. Fathi, M. Farzad, Effects of fly ash and TiO_2 nanoparticles on rheological, mechanical, microstructural and thermal properties of high strength self compacting concrete, Mech. Mater. 61 (2013) 11–27.
[7] L. Gustavsson, A. Joelsson, Life cycle primary energy analysis of residential buildings, Energy Build. 42 (2010) 210–220.
[8] G.A. Blengini, T. Di Carlo, The changing role of life cycle phases, subsystems and materials in the LCA of low energy buildings, Energy Build. 42 (2010) 869–880.
[9] C. Becchio, S.P. Corgnati, A. Kindinis, S. Pagliolico, Improving environmental sustainability of concrete products: investigation on MWC thermal and mechanical properties, Energy Build. 41 (2009) 1127–1134.
[10] B. Rosselló-Batle, A. Moià, A. Cladera, V. Martínez, Energy use, CO_2 emissions and waste throughout the life cycle of a sample of hotels in the Balearic Islands, Energy Build. 42 (2010) 547–558.
[11] J. Goggins, T. Keane, A. Kelly, The assessment of embodied energy in typical reinforced concrete building structures in Ireland, Energy Build. 42 (2010) 735–744.
[12] A. Bilodeau, V. Sivasundaram, K.E. Painter, V.M. Malhotra, Durability of concrete incorporating high volumes of fly ash from sources in US, ACI Mater. J. 91 (1994) 3–12.
[13] C. Shi, J. Qian, High performance cementing materials from industrial slags: a review, Resour. Conserv. Recycl. 29 (2000) 195–207.
[14] M. Tokyay, Characterization of Turkish Fly Ashes, Turkish Cement Manufacturers Associations, Ankara, 1998 (p. 70).
[15] A. Bilodeau, V.M. Malhotra, High-volume fly ash system: concrete solution for sustainable development, ACI Mater. J. 97 (2000) 41–48.
[16] V.M. Malhotra, Superplasticized fly ash concrete for structural applications, Concr. Int. 8 (1990) 28–31.
[17] N. Bouzoubaa, M. Laclemi, Self-compacting concrete incorporating high volumes of Class F fly ash: preliminary results, Cem. Concr. Res. 31 (2001) 413–420.
[18] M. Nehdi, M. Pardhan, S. Koshowski, Durability of self-consolidating concrete incorporating high-volume replacement composite cements, Cem. Concr. Res. 34 (2004) 2103–2112.
[19] M.A. Smith, The economic and environmental benefits of increased use of pfa and granulated slag, Resour. Policy 1 (3) (1975) 154–170.
[20] C. Fava et al., in: Proceedings of the 3rd International RILEM Symposium on Self-Compacting Concrete, RILEM Publications S.A.R.L., Reykjavik, 2003, pp. 628–636.
[21] C. Kulakowski et al., Carbonation induced reinforcement corrosion in silica fume concrete, Constr. Build. Mater. 23 (2009). 11897–1195.
[22] M. Shekarchi et al., Transport properties in metakaolin blended concrete, Constr. Build. Mater. 24 (2010) 2217–2223.
[23] T. Ji, Preliminary study on the water permeability and microstructure of concrete incorporating nano-SiO_2, Cem. Concr. Res. 35 (2005) 1943–1947.
[24] B.W. Jo, C.H. Kim, G.H. Tae, Characteristics of cement mortar with nano-SiO_2 particles, Constr. Build. Mater. 21 (2007) 1351–1355.
[25] Y. Qing, Z. Zenan, K. Deyu, et al., Influence of nano-SiO_2 addition on properties of hardened cement paste as compared with silica fume, Constr. Build. Mater. 21 (2007) 539–545.
[26] K.L. Lin, W.C. Chang, D.F. Lin, Effects of nano-SiO_2 and different ash particle sizes on sludge ash-cement mortar, J. Environ. Manage. 88 (2008) 708–714.
[27] A. Nazari, S. Riahi, Splitting tensile strength of concrete using ground granulated blast furnace slag and SiO_2 nanoparticles as binder, Energy Build. 43 (2011) 864–872.
[28] W.B. Fuller, S.E. Thompson, The laws of proportioning concrete, Trans. Am. Soc. Civ. Eng. 33 (1907) 222–298.
[29] A.H.M. Andreasen, J. Andersen, Ueber die Beziehung zwischen Kornabstufung und Zwischenraum in Produkten aus losen Körnern [Mit einigen Experimenten], Kolloid-Zeitschrift 50 (1930) 217–228 (in German).
[30] H.J.H. Brouwers, H.J. Radix, Self-compacting concrete: theoretical and experimental study, Cem. Concr. Res. 35 (2005) 2116–2136.
[31] S. Girish, R.V. Ranganath, Jagadish Vengala, Influence of powder and paste on flow properties of SCC, Constr. Build. Mater. 24 (2010) 2481–2488.
[32] ACI Committee 237Self-consolidating Concrete, ACI 237R-07, American Concrete Institute, Farmington Hills, 2007.
[33] S. Nagataki, H. Fujiwara, Self-compacting property of highly-flowable concrete, in: V.M. Malhotra (Ed.), Am Concr Inst SP 154 301–14 June, 1995.
[34] K.H. Khayat, Workability, testing and performance of self-consolidating concrete, ACI Mater. J. 96 (1999) 346–353.
[35] EFNARC, Specification & guidelines for self-compacting concrete, English ed. Norfolk (UK): European Federation for Specialist Construction Chemicals and Concrete Systems, 2002 (February).
[36] BS 1881-116, Testing concrete, Method for determination of compressive strength of concrete cubes, 1983.
[37] ASTM C696-96, Standard test method for splitting tensile strength of cylindrical concrete specimens, Annual Book ASTM Standard, vol. 4(04.02), 2001.
[38] ASTM C293Standard Test Method for Flexural Strength of Concrete (Using Simple Beam With Center-Point Loading), ASTM, Philadelphia, PA, 2001.
[39] K. Audenaert, Transport mechanismen in zelfverdichtend beton in relatie met carbonatatie en chloride penetratie (Ph.D. thesis), Ghent University, Ghent, 2006.
[40] N. Diamantonis, I. Marinos, M.S. Katsiotis, A. Sakellariou, A. Papathanasiou, V. Kaloidas, M. Katsioti, Investigations about the influence of fine additives on the viscosity of cement paste for self-compacting concrete, Constr. Build. Mater. 24 (2010) 1518–1522.
[41] M.K. Mohammed, A.R. Dawson, N.H. Thom, Macro/micro-pore structure characteristics and the chloride penetration of self-compacting concrete incorporating different types of filler and mineral admixture, Constr. Build. Mater. 72 (2014) 83–93.
[42] M.H. Zhang, J. Islam, Use of nano-silica to reduce setting time and increase early strength of concretes with high volumes of fly ash or slag, Constr. Build. Mater. 29 (2012) 573–580.
[43] L. Senff, D. Hotza, W.L. Repette, V.M. Ferreira, J.A. Labrincha, Mortars with nano-SiO_2 and micro-SiO_2 investigated by experimental design, Constr. Build. Mater. 24 (2010) 1432–1437.
[44] W. Wongkeo, P. Thongsanitgarn, A. Ngamjarurojana, A. Chaipanich, Compressive strength and chloride resistance of self-compacting concrete containing high level fly ash and silica fume, Mater. Des. 64 (2014) 261–269.
[45] K. Behfarnia, N. Salemi, The effects of nano-silica and nano-alumina on frost resistance of normal concrete, Constr. Build. Mater. 48 (2013) 580–584.
[46] F. Sanchez, K. Sobolev, Nanotechnology in concrete – a review, Constr. Build. Mater. 24 (2010) 2060–2071.
[47] J. Puentes, G. Barluenga, I. Palomar, Effects of nano-components on early age cracking of self-compacting concretes, Constr. Build. Mater. 73 (2014) 89–96.
[48] R. Yu, P. Tang, P. Spiesz, H.J.H. Brouwers, A study of multiple effects of nano-silica and hybrid fibers on the properties of Ultra-High Performance Fiber Reinforced Concrete (UHPFRC) incorporating waste bottom ash (WBA), Constr. Build. Mater. 60 (2014) 98–110.
[49] M.H. Beigi, J. Berenjian, O. Lotfi Omran, A. Sadeghi Nik, I.M. Nikbin, An experimental survey on combined effects of fibers and nanosilica on the mechanical, rheological, and durability properties of self-compacting concrete, Mater. Des. 50 (2013) 1019–1029.
[50] Y. Qing, Z. Zenan, S. Li, C. Rongshen, J. Wuhan Univ. Technol.: Mater. Sci. Ed. 21 (3) (2008) 153–157.
[51] E.J. Garboczi, D.P. Bentz, Constr. Build. Mater. 10 (1996) 293–300.
[52] S. Grzeszczyk, G. Lipowski, Cem. Concr. Res. 27 (1997) 907–916.
[53] E. Fernandez, F.J. Gil, M.P. Ginebra, F.C.M. Driessens, J.A. Planell, S.M. Best, J. Mater. Sci. Mater. Med. 10 (1999) 223–230.
[54] F. Massazza, Cemento 84 (October–December) (1987) 359–382.
[55] National Material Advisory Board, Concrete Durability: A Multi-billion Dollar Opportunity, NMAB-437, National Academy Press, Washington, 1987.
[56] T. Ji, Preliminary study on the water permeability and microstructure of concrete incorporating nano-SiO_2, Cem. Concr. Res. 35 (2005) 1943–1947.